Optics & Laser Technology 61 (2014) 1–7

Contents lists available at ScienceDirect

Optics & Laser Technology

journal homepage: www.elsevier.com/locate/optlastec

Thermal refraction in ionic liquids induced by a train of femtosecond laser pulses

J.A. Nóvoa-López [a], E. López Lago [b,*], M. Domínguez-Pérez [c], J. Troncoso [d], L.M. Varela [e], R. de la Fuente [b], O. Cabeza [c], H. Michinel [a], J.R. Rodríguez [e]

[a] Area de Óptica, Facultade de Ciencias de Ourense, Universidade de Vigo, As Lagoas s/n, Ourense, 32004 Spain
[b] Grupo de Microóptica y Sensores de Frente de Onda, Departamento de Física Aplicada, Universidade de Santiago de Compostela, Campus Vida s/n, E-15782 Santiago de Compostela, Spain
[c] Grupo Mesturas, Facultade de Ciencias, Universidade de A Coruña, Campus A Zapateira s/n, E-15008 A Coruña, Spain
[d] Departamento de Física Aplicada, Universidad de Vigo, Facultad de Ciencias, Campus As Lagoas, 32004 Ourense, Spain
[e] Grupo de Nanomateriales y Materia Blanda, Departamento de Física de la Materia Condensada, Universidade de Santiago de Compostela, Campus Vida s/n, E-15782 Santiago de Compostela, Spain

ARTICLE INFO

Article history:
Received 14 November 2013
Received in revised form
24 January 2014
Accepted 27 January 2014
Available online 17 February 2014

Keywords:
Ionic liquids
Nonlinear refraction
Thermal lens effect

ABSTRACT

The Z-scan technique is used to characterize the nonlinear refraction induced by a train of ultrashort laser pulses (80 fs, repetition rate 80.75 MHz) for a set of ionic liquids as a function of their structural parameters such as cation, anion type and alkyl chain length in the cation. The nonlinear refractive index change is originated by linear absorption processes which cause a nonlocal and inhomogeneous increase of temperature in the irradiated region of the sample that behaves as a thermal lens. The thermal refraction, according to the thermal lens model, is mainly related to three physical properties of the medium, which are the absorption at the excitation wavelength, the thermal conductivity and the thermo-optic coefficient. We explore the influence of anions and cations on these properties and on the thermal lens strength. The cationic influence was the object of study for the ILs based on the 1-butyl-3-methyl-imidazolium cation. The anionic influence was studied for the ILs based on the bis(trifluoromethylsulfonyl)imide anion. The obtained results show that both cation and anion affect significantly the thermal lens strength. The thermal refraction is 1.6 times higher in 1-butyl-3-methyl-imidazolium chloride than in 1-butyl-3-methyl-imidazolium bis(trifluoromethylsulfonyl)imide, and 3.3 times higher in trihexyl(tetradecyl)phosphonium bis(trifluoromethylsulfonyl)imide than in 1-butylpyridinium bis(trifluoromethylsulfonyl)imide. Optical absorption at 810 nm is influenced by both ionic parts, whereas the anion hardly determines the magnitude of the thermal conductivity.

1. Introduction

The term ionic liquid (IL) [1] refers to an organic salt that melts below 100 °C, although some of them, the so-called Room Temperature Ionic Liquids (RTIL(s)), are already liquid at room temperature. They are constituted by an organic cation, and an organic or inorganic anion which may be mono or polyatomic. The cation defines the family and usually contains N or P atoms and one or more linear alkyl chains, whereas the anion nature is quite varied. They are identified by the cation name followed by the anion name. When using shortened notation, the cation and the anion names are usually put into brackets. In this case, the alkyl chains are denoted as C_n, where C is the carbon atom symbol and n stands for the number of carbon atoms that the alkyl chain incorporates, i.e. the alkyl chain length.

Their singular properties make them interesting for a wide set of applications in many fields such as nuclear industry, photochemistry, renewable energy, nanotechnology and so on [2]. These properties may be easily tuned by an adequate anion and cation selection or mixing two or more IL(s). Thousands of scientific works have been published dealing with their physical and chemical properties and different technological applications. Nevertheless, few studies have explored their suitability for the fabrication of photonic components, where the knowledge of optical properties, such as chromatic dispersion, thermal refraction, linear and nonlinear absorption, and reflectivity, among others, is of crucial interest for the correct operation of a photonic device (see for example [3–5]). One of the best known optical properties is the refractive index and its variation with temperature, but most published studies obtain it at the yellow

* Corresponding author. Tel.: +34 981813518; fax: +34 981813534.
E-mail address: elena.lopez.lago@usc.es (E. López Lago).

http://dx.doi.org/10.1016/j.optlastec.2014.01.017
0030-3992

line of the sodium spectrum (λ_D=589.3 nm) [6,7]. For various optical applications, it is essential to know the refractive index properties of ionic liquids at other operational wavelengths, particularly those corresponding to the emission of the most common laser sources.

Nowadays, the availability of pulsed lasers allows reaching irradiances at a level high enough to generate nonlinear optical effects in materials, with important applications in optical switching, beam steering and so on [8]. In isotropic and homogeneous media, the most efficient optical nonlinearity is usually the Kerr effect, but in certain conditions other phenomena can arise, such as the thermal lens effect [9,10]. This latter is more relevant in liquids than in solids. Generally, in liquids, it causes a decrease of the refractive index, proportional to the induced change in temperature. On the contrary, the Kerr nonlinearity in transparent materials generates an increase of the refractive index proportional to the irradiance of the optical pulse. When these two effects coexist, the thermal lens one usually dominates [9], in particular once the steady state is reached. Thermal lensing becomes important if the pulse duration exceeds several nanoseconds or, even with shorter pulses, if the temporal interval between two consecutive pulses is less than the thermal relaxation time of the media. Thermal effects have been extensively studied since the 1960s and different models have been developed to describe them [11–13]. Thermal lens measurement has important applications in optical limiting [14] and laser technology [15,16] but also in spectroscopy [17], calorimetry [18] and microscopy [19] where the properties of the solvent determine, among others, the sensitivity of the measurement.

Z-scan, an experimental technique developed in 1989, is very appropriate to determine the parameters that characterize the nonlinear refraction of both thermal and optical origin [20]. For an adequate interpretation of the Z-scan measurement, the key factor is choosing the suitable theoretical model to describe the refractive index change, since Kerr and thermo-optical effects are triggered by different physical mechanisms [21]. The Z-scan has been applied to the characterization of solid and liquid samples using different laser sources, both pulsed and CW lasers. Recently, the Z-scan has been employed to characterize the thermal refraction in some 1-methyl-imidazolium-based ionic liquids, such as $[C_4C_1im][BF_4]$, $[C_4C_1im][PF_6]$ [22], $[C_2C_1im][Tf_2N]$, $[C_2C_1im][CF_3CO_2]$, $[C_4C_1im][CF_3CO_2]$ [23], ionic liquids based on the $[PR_4]$ cation combined with different metallic anions [24,2] and IL(s) of the 1-methylpirrolidine family [25]. It is well known that the refractive index change induced by high repetition lasers or CW laser is in general a nonlocal effect. The influence on the degree of nonlocality of the anion and of the alkyl chain length of the cationic part in methylimidazolium-based IL(s) has been analyzed in Ref. [26] by means of Z-scan data at 820 nm. The authors analyze the anionic influence combining the cation $[C_4C_1im]^+$ with $[Tf_2N]^-$, $[BF_4]^-$ and $[PF_6]^-$ anions. The effect of the cation was studied for $[Tf_2N]^-$-based systems, varying the cation alkyl chain length, n ($[C_nC_1im][Tf_2N]$, n=4,6,8,10,12). They found that the strength of nonlocality is mainly dependent on the anion involved in the IL and that the changes in the alkyl chain are not significant, at least for the set of measured IL(s). A similar study was carried out for laser excitation tuned at 410 nm [27], where the authors observed that the strength of the thermal refraction was two orders of magnitude higher than that at 820 nm. Thermal lens signals were also measured in $[C_4C_1im][BF_4]$, $[C_4C_1im][PF_6]$ $[C_nC_1im][Tf_2N]$ (n=2,4,5,6,8) using the dual-wavelength pump/probe configuration thermal lens spectrometer [28]. Essentially, the sample was excited by a pump beam derived from an argon laser (λ=514.5 nm), and the photoinduced thermal lens was measured by a He–Ne probe laser (λ=632.8 nm).

This work is aimed at a systematic study of the influence of thermal lens effects in a set of ionic liquids which belong to different families of IL(s) (methyl-imidazolium, pyridinium, methyl-pyperidinium, methyl-pyrrolidinium, tetra-alkyl-phosphonium, and trialkyl-sulphonium families). We analyze the thermal effect strength as a function of the cation, anion nature, and the length of the alkyl chains present in the cation. The paper is structured as follows: Section 2 is dedicated to the introduction to the IL(s), which are the object of this study, as well as to the description of the used equipment, paying special attention to the home made Z-scan setup. In Section 3, we revisit the characteristics of light propagation in isotropic and homogeneous media under the thin-sample approximation, when the Kerr or thermal lens effect develops in the medium, and we stress the main differences between them. We also revise the characteristics of the Z-scan curves when the nonlinear refraction is generated by one of these mechanisms. In Section 4, we present and analyze the results of the characterization and, finally, in Section 5 we present the conclusions derived from the analysis.

Table 1
List of ionic liquids studied together with their optical absorption coefficients at 810 nm, α_0 (m^{-1}). Thermal conductivity, κ (W/mK), of some ionic liquids is also given at 298 K: (1) this work, (2) extracted from ILThermo Database, (3) extracted from [29]. The uncertainty associated with the optical absorption coefficient is less than 3%. The uncertainties for the thermal conductivity values measured in this work are about 10%.

Short name	Long name	α_0	κ
$[C_2C_1im][Tf_2N]$	1-Ethyl-3-methylimidazolium bis(trifluoromethylsulfonyl)imide	17.3	0.130(2)
$[C_2C_1im][BF_4]$	1-Ethyl-3-methylimidazolium tetrafluoroborate	8.1	0.170(1)
$[C_2C_1im][EtSO_4]$	1-Ethyl-3-methylimidazolium ethyl sulfate	2.5	0.178(3)
$[C_4C_1im][Tf_2N]$	1-Butyl-3-methylimidazolium bis(trifluoromethylsulfonyl)imide	4.9	0.128(2)
$[C_4C_1im][BF_4]$	1-Butyl-3-methylimidazolium tetrafluoroborate	1.5	0.176(1)
$[C_4C_1im][SbF_6]$	1-Butyl-3-methylimidazolium hexafluoroantimonate	3.6	NA
$[C_4C_1im][MetSO_4]$	1-Butyl-3-methylimidazolium methylsulfate	5.8	NA
$[C_4C_1im][MetFSO_3]$	1-Butyl-3-methylimidazolium triflate	4.3	0.147(2)
$[C_4C_1im][Cl]$	1-Butyl -3-methylimidazolium chloride	58.4	NA
$[C_4C_1im][N(CN)_2]$	1-Butyl-3-methylimidazolium dicyanamide	8.3	NA
$[C_6C_1im][Tf_2N]$	1-Hexyl-3-methylimidazolium bis(trifluoromethylsulfonyl)imide	5.9	0.127(2)
$[C_6C_1im][BF_4]$	1-Hexyl-3-methylimidazolium tetrafluoroborate	0.3	0.158(1)
$[C_6C_1im][Br]$	1-Hexyl-3-methylimidazolium bromide	5.1	NA
$[C_8C_1im][BF_4]$	1-Octyl-3-methylimidazolium tetrafluoroborate	<0.3	0.157(1)
$[C_8C_1im][Br]$	1-Octyl-3-methylimidazolium bromide	25.8	NA
$[C_{10}C_1im][BF_4]$	1-Decyl-3-methylimidazolium tetrafluoroborate	0.3	0.198(1)
$[C_4C_1Pip]$ $[Tf_2N]$	1-Butyl-1-methylpiperidinium bis(trifluoromethylsulfonyl)imide	4.5	NA
$[C_4Py]$ $[Tf_2N]$	1-Butylpyridinium bis(trifluoromethylsulfonyl)imide	4.3	NA
$[C_4C_1Pyrr]$ $[Tf_2N]$	1-Butyl-1-methylpyrrolidinium bis(trifluoromethylsulfonyl) imide	3.9	0.125(2)
$[C_6C_6C_6C_{14}P][Tf_2N]$	Trihexyl(tetradecyl)phosphonium bis(trifluoromethylsulfonyl) imide	7.4	0.144(2)
$[C_2C_2C_2S][Tf_2N]$	Triethylsulphonium bis(trifluoromethylsulfonyl)imide	13.6	NA

2. Materials and experiments

The ionic liquids used in this work are listed in Table 1 as well as the short names used throughout the present paper. They were selected because they include some of the most common anions and cations. In order to evaluate the influence of the chemical structure of both the cation and anion, most of the measured ionic liquids can be segregated in two groups defined by a common ion: one of them is characterized by the presence of the $[NTf_2]^-$ anion and the other by the $[C_4C_1im]^+$ cation. Thus, the effect in the nonlinear optical properties of changing the cation or anion may be easily evaluated. Nevertheless, the effect of the chain length in the methyl-imidazolium cation was also studied for $[BF_4]^-$ anions. $[C_6C_1im][Br]$, $[C_8C_1im][Br]$ and $[C_2C_1im][EtSO4]$ were also measured due to their importance and availability. Ionic liquids $[C_6C_1im][NTf_2]$, $[C_4C_1im][SbF_6]$, $[C_4C_1im][MetSO_4]$, and $[C_4C_1im][MetFSO_3]$ were purchased from Solvent Innovation, whereas the other ionic liquids were purchased from IoLiTec. In order to remove volatile compounds from the liquids, all of them were kept at 333 K under vacuum for 48 h before starting the measurements. It should be noted that the fusion temperature of $[C_4C_1im][Cl]$ is well above room temperature about 333.15 K; nevertheless, we could manage to measure it in liquid state because it is highly metastable and, once melted, it remains as an undercooled liquid for several weeks at room temperature. The purity of the IL(s) is higher than 99% except for $[C_4\ C_1im][N(CN)_2]$, $[C_6C_6C_6C_{14}P]$ $[NTf_2]$, $[C_2C_1im]$ $[BF_4]$ and $[C_{10}C_1im][BF_4]$, which is higher than 98%.

The experiments have been conducted with a typical Z-scan setup, as the shown in Fig. 1a, under the conditions that have been specified in Table 2. Pulses of $\tau_0=80$ fs (FWHM) are delivered by a Ti:sapphire oscillator at $\lambda_0=810$ nm with a repetition rate of 80.75 MHz. The laser beam was focused by a positive lens (L) to a Gaussian spot with a 17 μm radius (at $1/e^2$ intensity) measured by the knife-edge method [29]. A linear polarizer (LP) kept fixed the polarization state of the beam. The mean optical power at the input of the sample is varied by rotating a half wave plate (WV) placed before the linear polarizer. A 1 mm quartz cell filled with the IL is moved with a motorized translation platform from a position ahead the focus towards a position behind it, with a 1 mm step. The power transmitted through a circular aperture of 1.6 mm diameter (S) is collected and measured by a photodiode detector (D). All measurements have been performed under the same conditions except for the input mean power that varies from 170 mW to 1.5 W to ensure that the induced nonlinear phase meets the requirements of the Z-scan technique. Fig. 1b shows a photograph of the experimental setup with each labeled optical element.

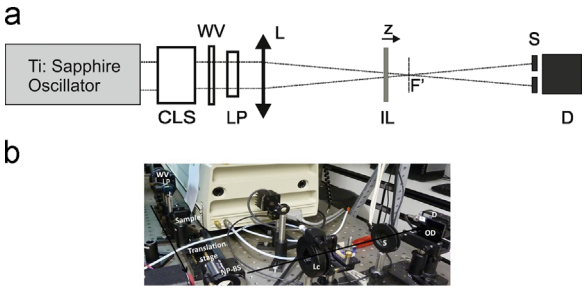

Fig. 1. (a) Experimental setup for the Z-scan measurement. The laser pulses are delivered by a Ti: Sapphire oscillator; a system of lens (CLS) is used to collimate the beam. A half wave plate (WV) followed by a linear polarizer (LP) allows varying the input power level. Lens (L) focuses the beam, its back focal point is at F'. The position of the cell with the ionic liquid (IL) is moved from a position ahead the focus (F') towards a position behind by means of a translation stage (not drawn for simplicity). A slit (S) in the far-field selects only the central part of the beam. The power transmitted by S is collected by the head of the detector D. (b) Picture of the experimental setup: half wave plate (WV), linear polarizer (LP), positive lens (L), non polarizing beam-splitter (NP-BS) for changing the direction of a portion of the optical beam by 90°, positive lens (Lc) used to ensure that all the light enters the detector head (only in open aperture experiments), slit (S), optical density (OD) and detector (D).The second non polarizing beam-splitter (NP-BS) is used to share the laser source with other experiments.

Table 2
Conditions of the Z-scan experiment.

w_0 (μm)	z_0 (mm)	L (mm)	P (W)	τ_0 (fs)	fr (MHz)	t (s)
17	1.1	1	0.17–1.7	80	80.75	> 1

The absorption coefficient was calculated starting from the transmittance data measured with a Perkin Elmer Lambda 25 spectrometer. The thermal conductivity has been measured by the F5 Technology Lambda System 2 that uses the well-known hot wire technique [30] and it has a reproducibility of ± 1%. To regulate the sample temperature we use a Haake F3 thermostat. The temperature of the sample is measured by an internal thermometer calibrated with an ANTON PAAR DT 100-30, with a resolution better than 0.1° C.

3. Theory

3.1. Nonlinear refraction

A TEM_{00} fundamental mode of a laser beam may be accurately described by a Gaussian function; therefore, the electric field may be expressed as

$$E_i(x,y,z)=E_0 e^{-\frac{x^2+y^2}{w(z)^2}} e^{i\phi(x,y,z)} \tag{1}$$

z being the propagation direction, E_0 the maximum value of the Gaussian amplitude, $w(z)$ the width of the beam along propagation at the $1/e^2$ intensity, and ϕ standing for the phase accumulated by the beam under propagation.

Under the thin sample approach, the linear diffraction and the nonlinear refraction effects in amplitude can be neglected. This approach is valid if the length of the medium, L, is shorter than the Rayleigh distance of the beam defined as $\pi w_0^2/\lambda_0$, where w_0 is the minimum width of the beam which is considered located at the input of the medium, *i.e.* $z=0$ [31]. Then, at the output of the medium ($z=L$) the shape of the amplitude of the electric field remains unchanged, except attenuation, whereas the optical beam suffers a phase change, $\Delta\phi$. Under this condition, the field at the output of the medium is well described as:

$$E_0(x,y,L)=E_i(x,y,0)e^{i\Delta\phi(x,y,L)}e^{-\frac{\alpha_0}{2}L} \tag{2}$$

$$\Delta\phi(x,y,L)=\frac{2\pi}{\lambda_0}n'(x,y,L)L_{eff} \tag{3}$$

where λ_0 is the reference wavelength (central wavelength of the pulse), $n'(x,y,L)$ carries information about the linear and nonlinear terms of the refractive index $n(x,y)$, and L_{eff} the effective length defined as [20]:

$$L_{eff}=\frac{1-e^{-\alpha_0 L}}{\alpha_0} \tag{4}$$

where α_0 is the linear absorption coefficient at λ_0. In transparent materials, where optical losses are negligible, L_{eff} is equal to L.

In homogeneous, isotropic materials and at low power/irradiance, n has a value, n_0, which depends only on the wavelength. When the power and/or the irradiance of the beam are high enough to develop nonlinear refraction effects, the medium turns locally inhomogeneous so the refractive index may be described as

$$n(x,y)=n_0+\Delta n(x,y) \tag{5}$$

where $\Delta n(x,y)$ stands for the spatial variation of the refractive index. Its origin can be attributed to different mechanisms whose excitation depends on the characteristics of the laser pulses. As mentioned previously, the use of high repetition ultrashort laser pulses can lead to the generation of these two effects, the electronic Kerr effect and the thermal lens effect.

The electronic Kerr effect induces a variation in the refractive index, which is proportional to the input irradiance, $I_i(x,y)$ [9]:

$$n(x,y) = n_0 + n_2|E_i(x,y)|^2 = n_0 + \gamma I_i(x,y) \quad (6)$$

where n_2 is known as the nonlinear refractive index, $\gamma = n_2/(2\varepsilon_0 c n_0)$. c is the speed of light at vacuum and ε_0 the permittivity of the vacuum; n_2 can be positive (so that the refractive index is higher in the irradiated region) or negative (the refractive index decreases in the irradiated area). Due to the inhomogeneous profile of the refractive index, the medium acts as a convergent ($n_2 > 0$) or divergent lens ($n_2 < 0$) inducing self-focusing or self-defocusing of the beam, respectively. The Kerr effect can be originated by different physical mechanisms with different temporal responses (electronic, nuclear or molecular orientation) [9]. Under the conditions of this work, the most likely origin of the nonlinearity is the electronic one, since the rise-up time with this mechanism is shorter than the duration of pulses delivered by the laser source used in the experiments. Indeed, the electronic response of the media is considered instantaneous; the maximum rise-up time is of few femtoseconds and the relaxation or decay time takes values ranging from few femtoseconds to hundreds of femtoseconds [9,34]. The nuclear response has build-up times ranging between 10 fs and 1 ps [10], but in organic materials its contribution is expected to be much smaller than that of the electronic response [35]. The molecular orientation mechanism is characterized by longer build-up times between 1 and 10 ps, so the generated effect cannot be experienced by the generative pulse. On the other hand, the three mechanisms (electronic, nuclear and molecular orientation) have decay times shorter than the temporal interval between pulses (about 12 ns), preventing cumulative effects [34].

When the thermal lens effect is responsible for the refractive index variation, the thermal refraction is caused by the heating of the medium due to linear or nonlinear absorption processes. For low absorbing materials, the variation of the refractive index is well described by:

$$n(x,y) = n_0 + \Delta n(x,y) = n_0 + \frac{dn}{dT}\Delta T(x,y) \quad (7)$$

where (dn/dT)stands for the thermo-optic coefficient and $\Delta T(x,y)$ refers to the nonlocal temperature change which depends on the optical fluence, instead of on the optical irradiance [20]. The sign of (dn/dT) determines the focusing or defocusing of the beam as n_2 or γ do.

Although apparently both effects are described by a refractive index which depends on the spatial transversal coordinates, there are important differences between them. The electronic Kerr nonlinearity is local and fast. It is originated due to distortions in the electronic cloud due to the electric field that induces changes in the optical susceptibility of the medium and gives rise to a nonlinear optical polarization. The thermal effect has a slow and accumulative response which, in general, is nonlocal due to heat conduction. In transparent media, including liquids, the Kerr effect is generally characterized by an $n_2 > 0$. On the contrary, thermal effects in liquids used to cause a decrease of the refractive index. If the two effects coexist, thermal nonlinearities usually prevail over the Kerr effect, which may be from one to several orders of magnitude lower [9,10].

The efficiency of these mechanisms depends strongly on the characteristics of the laser source which generates the train of pulses. In this work we use a Ti:Sapphire oscillator which delivers 80 fs pulses every 12.38 ns (repetition rate of 80.75 MHz). These conditions benefit the occurrence of the two above-mentioned effects since the temporal interval between pulses is smaller than the thermal characteristic time of the medium, t_c, given by

$$t_c = \frac{w(z)^2}{4D} = \frac{w(z)^2}{4}\frac{\rho C_p}{\kappa} \quad (8)$$

$w(z)$ being the beam width and D the thermal diffusivity of the medium, usually with values of about 10^{-6} m^2/s. Thermal diffusivity quantifies how quickly the material conducts heat in relation to its volumetric heat capacity given by ρC_p (κ is the thermal conductivity, ρ is the density and C_p the specific heat capacity at constant pressure). t_c measures the required time by the material to recover its initial thermal state.

3.2. Z-scan characterization of thermal effects

The Z-scan technique, proposed by Sheik-Bahae in the late 1980s, is particularly useful for the characterization of the nonlinear refractive index change in optical materials, due to its simplicity and accuracy [20]. It allows retrieving the parameters that characterize the nonlinearity starting from the transmitted power variation through a far-field aperture as a function of the relative distance, Δz, between the sample position and the focus of the optical system. The transmittance curve exhibits a maximum (peak) and a minimum (valley) whose relative position is related to the sign of the nonlinearity. If the peak precedes the valley nonlinearity is negative and, conversely, a valley which precedes a peak is indicative of positive nonlinearity. To explain this behavior, without loss of generality, let us consider a medium that originates a negative thermal lens yielding a $\Delta n < 0$. Let $z=0$, the location of focal point of the positive lens (L in Fig. 1a and b). When the sample is far from the focus, |Δz|â¹¢0, the nonlinear effects are negligible since the fluence is too low, so the beam divergence at the slit plane transmitted power by the slit (S) are independent of the sample position. As the sample gets close to the focus, the fluence increases and a negative thermal lens is created in the medium. If the sample is before the focus ($\Delta z < 0$) the thermal lens shifts the focalization point of the beam towards $z > 0$. Consequently, the beam divergence at the slit plane is lower and therefore the transmitted power measured by the detector is higher than the one detected in the linear case. On the contrary, when the sample is placed after the focus, ($\Delta z > 0$) the negative lens increases the divergence of the beam resulting in a decrease of the transmitted power.

The peak-to-valley distance, ΔZ_{pv}, provides important information about the origin of the nonlinear refraction. Sheik Bahae formalism predicts that for a Kerr nonlinearity, this value is almost constant and close to $1.7z_0$, z_0 being the Rayleigh length of the beam [20]. Thermal effects give rise to higher values of ΔZ_{pv}, depending on the strength and origin of the thermal lens as it has been reported in the literature [13,31–33]. It has been shown that ΔZ_{pv} changes with the irradiation time until reaching an asymptotic value depending on the order of the involved absorption processes. The asymptotic value is achieved for irradiation times longer than $100t_c$.

Different models have been developed for predicting the behavior of the transmittance curve in the presence of thermal effects. In this paper we adopt the model used by Falconieri in Ref. [33], which accounts for the use of high repetition rate lasers. Although Falconieri's model incorporates multiphoton absorption processes as possible causes of the temperature increase, we consider that the heating of the medium is only originated by linear absorption processes only. Under this assumption, the

normalized transmittance behavior is described by

$$T(z) = 1 + \theta \tan^{-1}\left[\frac{2(z/z_0)}{[9+(z/z_0)^2](1+(z/z_0)^2)/2\tau + [3+(z/z_0)^2]}\right] \quad (9)$$

where θ is given by

$$\theta = -\frac{P\alpha_0}{\lambda_0 \kappa} L_{eff} \frac{dn}{dT} \quad (10)$$

P being the laser power, and τ standing for t/t_c, where t is the irradiation time and t_c the thermal characteristic time of the medium, defined in Eq. (8).

It should be mentioned that Falconieiri's model allows the study of the temporal dynamics of the refractive index change. Short irradiation times followed by light-off periods higher than t_c, minimize the thermal lens contribution to the Z-scan data and allow the isolation of the fast optical nonlinearities.

4. Results and discussion

All the Z-scan curves exhibit a defocusing behavior compatible with a negative thermo-optic coefficient. Eq. (9) has been fitted to each experimental curve. These fits return θ and z_0. The fitted value of z_0 is a 25% higher than the one shown in Table 2 calculated using the measured value of w_0. The corresponding value of w_0 is 19 μm, very close to the value given in Table 2, which is 17 μm. The peak to valley distance, Δz_{pv}, takes values between 5 ± 1 mm, which suggests a nonlinearity of thermal origin attending to the ratio $\Delta z_{pv}/z_0$. Table 3 summarizes the fit parameters whose relative uncertainties are about 5% and 2% respectively, which should be added to the uncertainty of the Z-scan measurement. As example, some normalized transmission curves are shown in Fig. 2, together with the fitting of Eq. (9) to the experimental data.

The normalized thermal refraction, given by θ/P in Table 3, is highly sensitive to the anionic part of the IL: the achieved values vary from 0.49 for $[Tf_2N]^-$ (practically transparent at 810 nm) to 0.85 for $[Cl]^-$ (50 times more absorbent). The linear optical absorption coefficients at 810 nm, α_0, are shown in Table 1. The influence of the cation is also studied by keeping $[Tf_2N]^-$ as anion. In this case, we have obtained values which varied from 0.3 for $[C_4C_1Py]$ $[Tf_2N]$ to 1.00 for $[C_6C_6C_6C_{14}P]$ $[Tf_2N]$. In Table 4, the IL(s) with common cation and anion have been ordered from weaker to stronger thermal refraction strength.

Table 3
Average power (P), fitted values of the parameter θ of Eq. (9), corresponding to each of the obtained Z-scan curves. The averaged ratio θ/P allows making a comparison between the strength of the nonlinear refraction observed in the ionic liquids.

Short name	P (W)	θ	θ/P (W^{-1})	$-dn/dT$ (K^{-1})
$[C_2C_1im][Tf_2N]$	1.05	0.67	0.64	4×10^{-6}
$[C_2C_1im][BF_4]$	1.08	0.65	0.60	1.1×10^{-5}
$[C_2C_1im][EtSO_4]$	1.07	0.52	0.47	2.8×10^{-5}
$[C_4C_1im][Tf_2N]$	1.08	0.53	0.49	1.1×10^{-5}
$[C_4C_1im][BF_4]$	1.08	0.55	0.51	4.8×10^{-5}
$[C_4C_1im][SbF_6]$	0.39	0.22	0.57	NA
$[C_4C_1im][MetSO_4]$	0.3	0.21	0.70	1.9×10^{-5}
$[C_4C_1im][MetFSO_3]$	0.38	0.22	0.58	NA
$[C_4C_1im][Cl]$	0.68	0.58	0.85	NA
$[C_4C_1im][N(CN)_2]$	0.41	0.25	0.61	NA
$[C_6C_1im][Tf_2N]$	1.06	0.55	0.52	0.9×10^{-5}
$[C_6C_1im][BF_4]$	1.48	0.88	0.60	2.5×10^{-4}
$[C_6C_1im][Br]$	1.06	1.28	1.21	NA
$[C_8C_1im][BF_4]$	1.1	0.89	0.81	3.4×10^{-4}
$[C_8C_1im][Br]$	1.08	1.09	1.01	NA
$[C_{10}C_1im][BF_4]$	1.03	0.86	0.83	4.5×10^{-4}
$[C_4C_1Pip]$ $[Tf_2N]$	0.39	0.24	0.60	NA
$[C_4Py]$ $[Tf_2N]$	0.39	0.12	0.30	NA
$[C_4C_1Pyrr]$ $[Tf_2N]$	0.59	0.30	0.5	1.3×10^{-5}
$[C_6C_6C_6C_{14}P][Tf_2N]$	0.42	0.42	1.00	1.5×10^{-5}
$[C_2C_2C_2S][Tf_2N]$	0.36	0.14	0.39	NA

Table 1 also shows the thermal conductivity at 298.3 K for some of the IL(s) under study. Some of them, those labeled with (1) have been measured for this work, the IL(s) labeled with (2) have been extracted from [36] and the thermal conductivity of $[C_2C_1im]$ $[EtSO_4]$ has been obtained from [37]. The thermal conductivity of $[C_nC_1im]$ [X] ([X]: $[BF_4]^-$ or $[Tf_2N]^-$) decreases in general with the alkyl chain length except for $[C_{10}C_1im]$ $[BF_4]$ which has a higher value, close to the thermal conductivity of $[C_2C_1im]$ $[BF_4]$. Such a non-monotonic behavior of this property with the alkyl chain length is also obtained with the data given in reference [26] related to the $[Tf_2N]^-$. Our results confirm that the nature of the cation has only a slight influence on the thermal conductivity of the IL, and that the anion exerts the strongest influence on this physical property, as it has been observed in other physical properties. In particular, $[BF_4]^-$ anion gives rise to higher thermal conductivities than $[Tf_2N]^-$ when combined with the same cation.

The absorption coefficient, see Table 1, seems to decrease as the alkyl chain length increases for the $[C_nC_1im][BF_4]$ ionic liquids, but we could not determine it for the $[C_8C_1im]$ $[BF_4]$. The reason is that this family of ionic liquids is highly transparent at 810 nm and an absorption coefficient around 0.3 m^{-1} produces absorbance values with path lengths of 1 cm, which are very close to the threshold of the spectrometer. An accurate measurement should be carried out with thicker cells, but the available spectrometer does not hold cells thicker than 1 cm. This growth pattern has not been observed with the $[Tf_2N]^-$, neither in the results derived from our work nor in those shown in reference [26]. In Table 4, IL(s) with a common cation $[C_4C_1im]^+$ and IL(s) with a common anion $[Tf_2N]^-$ have been ordered from lower to higher values of optical absorption.

It is important to note that the optical absorption measurements are very sensitive to the impurities content of the IL(s), even in very low proportions. Even the spectra of highly pure IL(s) coming from different synthesis processes may exhibit measurable differences, mainly in the UV region, but the tail may reach the vis and even IR spectral regions [38,39]. In this sense, although our samples were carefully handled and the impurities content proved to be low, one should take this factor as a possible contribution to the experimental uncertainties of our results.

The thermo-optic coefficient may be calculated by using the measured values of θ, α and κ in Eq. (7). We could determine the thermo-optic coefficient only for a subset of the studied IL(s). The thermo-optic coefficient of IL(s) based on $[C_nC_1im][BF_4]$ seems to increase (absolute value) as the alkyl chain does, and reaches values similar to those observed in other liquids such as castor oil ($(dn/dT) = -1 \times 10^{-5}\ K^{-1}$) [40], CS_2 ($(dn/dT) = -5 \times 10^{-4}\ K^{-1}$) [41], or $[C_4C_1im]$ $[PF_6]$ ($(dn/dT) = -8.1 \times 10^{-5}\ K^{-1}$) [22]. When $[Tf_2N]^-$ replaces $[BF_4]^-$, this tendency is not observed, since the thermo-optic coefficient of $[C_6C_1im][Tf_2N]$ presents a lower value than the one obtained with $[C_4C_1im][Tf_2N]$, in agreement with previously reported results [26].

It is worth mentioning that we carried out experiments in order to isolate the fast component of the optical nonlinearity (short irradiation times and long light-off periods compared to t_c), but the Z-scan curve was flat. This result means that, under the conditions of our experiments, the contribution of the electronic and nuclear optical nonlinearities to the Z-scan curves is negligible. On the other hand, Z-scan data taken with open aperture mode show no traces of nonlinear absorption processes in these ILs.

5. Conclusions

Thermal refraction was systematically characterized in a set of ionic liquids by means of the Z-scan technique, which has been

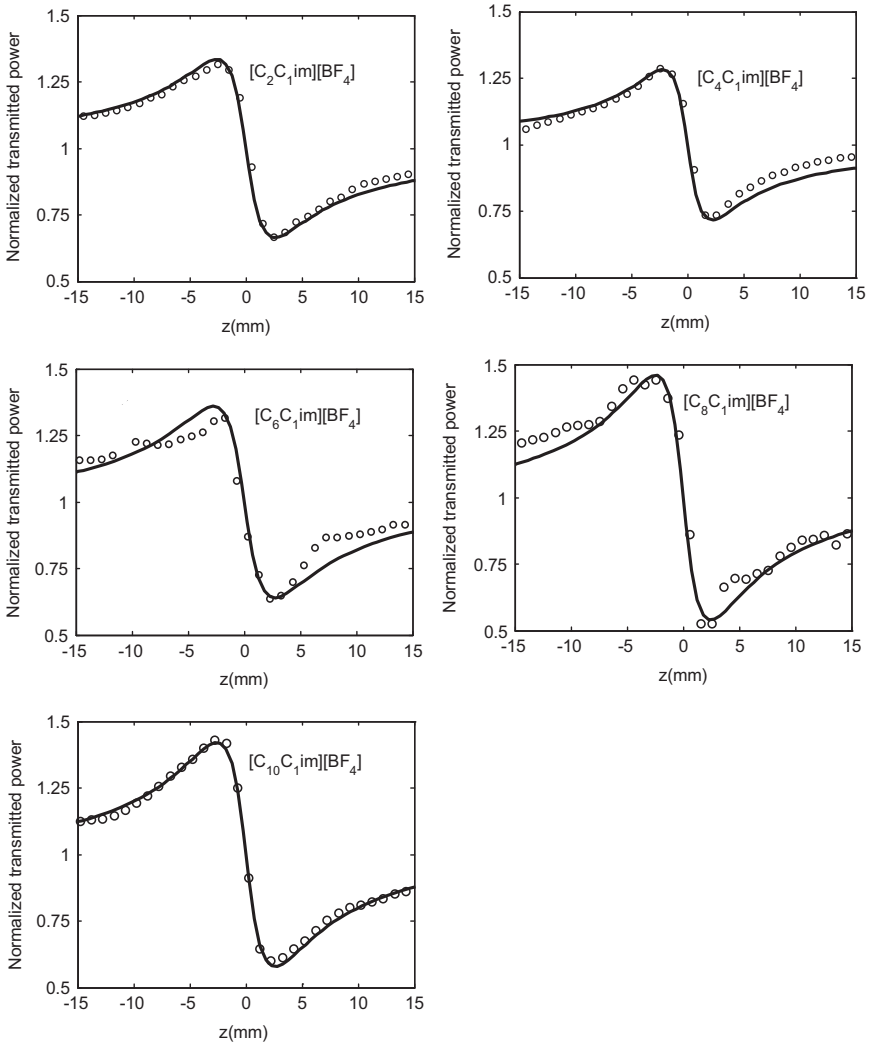

Fig. 2. Open circles: experimental Z-scan data corresponding to the five ionic liquids which differ only on the alkyl chain length $[C_nC_1im][BF_4]$. Continuous line: fitting of Eq. (9) to the experimental data. The corresponding average powers are shown in Table 3.

Table 4
From left to right, anions (top) and cations (bottom) have been ordered from lower to higher values of the measured normalized peak to valley amplitude and linear absorption coefficient; available thermal conductivities are also shown.

$[C_4C_1im]$ [anion]							
θ/P	**Tf_2N** (0.49)	**BF_4** (0.52)	**SbF_6** (0.57)	**MetFSO$_3$** (0.58)	**$N(CN)_2$** (0.61)	**$MetSO_4$** (0.75)	**Cl** (0.81)
α **(m^{-1})**	**BF_4** (1.5)	**SbF_6** (3.6)	**MetFSO$_3$** (4.3)	**Tf_2N** (4.9)	**$MetSO_4$** (5.8)	**$N(CN)_2$** (8.3)	**Cl** (58.4)
κ **(W/mK)**	(0.176)		(0.147)	(0.128)			
[Cation] $[Tf_2N]$							
θ/P	**C_4Py** (0.30)	**$C_2C_2C_2S$** (0.39)	**C_4C_1im** (0.49)	**C_4C_1Pyrr**(0.51)	**C_6C_1im** (0.52)	**C_4C_1Pyp** (0.60)	**C_2C_1im** (0.64)	**$C_6C_6C_6C_{14}P$** (1.00)
α **(m^{-1})**	**C_4C_1Pyrr** (3.9)	**C_4 Py** (4.3)	**C_4C_1Pyp** (4.5)	**C_4C_1im** (4.9)	**C_6C_1im** (5.9)	**$C_6C_6C_6C_{14}P$** (7.4)	**$C_2C_2C_2S$** (13.6)	**C_2C_1im** (17.3)
κ **(W/mK)**	(0.125)			(0.128)	(0.127)	(0.144)		(0.130)

carried out with a train of pulses delivered from a Ti:sapphire oscillator. The studied IL(s) were selected according to their molecular composition in order to find out how much it (cation, anion or alkyl chain length) governs the thermal phase shift experienced by a laser beam which propagates across these IL(s). Linear absorption and, when possible, thermal conductivity have been measured in order to determine their thermo-optic coefficient. Anion chemical nature was revealed as the factor which determines to a greater extent the behavior of the thermal conductivity, while absorption is dependent on both the cationic and anionic part of these compounds. Consequently, we have not found a clear and systematic relation between the thermal refraction strength and the structural parameters of the IL(s). It seems that bromide and chloride anions contribute to the enhancement of the thermal lens effect. Our results also point out that thermal lens signals are stronger for the phosphonium-based IL and weaker for 1-methylpyridinium-based IL, at least for IL(s) containing $[Tf_2N]^-$. In order to achieve conclusive results that support a theory for predicting the thermal lens behavior of an IL, further studies should be conducted, involving other anionic and cationic species as well as systematically exploring other properties such as thermal expansion, packing or molecular size. Work in

this direction is now in progress. A further rationale for the behavior of the Z-scan measurements demands the analysis of thermal conductivity and thermo-optic coefficient. To this end, direct measurements of the latter and an understanding of the former within the framework of the Eyring theory [42] are currently in progress.

Acknowledgment

The authors wish to thank the financial support from Xunta de Galicia through the Research Projects 10-PXI-103-294 PR, 10-PXIB-206-294 PR, K133131H64102, K044131H64502, CN2012/156, CN2012/227, as well as from the Galician Network on Ionic Liquids, REGALIS (CN 2012/120). All these research projects are co-funded by FEDER. JAN thanks University of Vigo for grant: Axudas predoutorais.

References

[1] Kokorin A, editor. Ionic liquids: theory, properties, new approaches. Intech: Zagreb, Croatia; 2011.
[2] Rogers RD, Seddon KR. Ionic liquids IIIB: fundamentals, progress, challenges and opportunities: transformations and processes. . Washington, DC: ACS Symposium Series; 2005.
[3] Calixto S, Sánchez-Morales ME, Sánchez-Marín FJ, Rosete-Aguilar M, Martínez Richa A, Barrera-Rivera KA. Optofluidic focus variable lenses. Appl Opt 2009;48:2308–10.
[4] Borra EF, Seddiki O, Eisenstein D, Hickson P, Seddon KR. Deposition of metal films on an ionic liquid as a basis of a lunar telescope. Nature 2007;447:979–81.
[5] Hu X, Zhang S, Lui Y, Qu C, Lu L, Ma X, et al. Electrowetting based infrared lens using ionic liquids. Appl Phys Lett 2011;99:213505.
[6] Tariq M, Forte PAS, Costa Gomes MF, Mayongia Lopes JN, Rebelo LPN. Densities and refractive indices of imidazolium-based and phosphonium-based ionic liquids: effect of temperature, alkyl chain length and anion. J Chem Thermodyn 2009;41(790–798).
[7] Pereiro B, Legido JL, Rodríguez A. Physical properties of ionic liquids based on 1-alkyl-3-methylimidazolium cation and hexafluorophosphate as anion and temperature dependence. J Chem Thermodyn 2007;39:1168–75.
[8] Resler DP, Hobbs DS, Sharp RC, Friedman LJ, Dorschner TA. High-efficiency liquid-crystal optical phased-array beam steering. Opt Lett 1996;21:689–91; Królikowski W, Kivshar YS. Soliton-based optical switching in waveguide arrays. J Opt Soc Am B 1996;13:876–87.
[9] Boyd RW. Nonlinear optics. Second edition. Amsterdam: Academic Press Inc; 2003.
[10] Christodoulides DN, Khoo IC, Salamo GJ, Stegeman GI, Van Stryland EW. Nonlinear refraction and absorption: mechanisms and magnitudes,. Adv Opt Photon 2010;2:60–200.
[11] Gordon JP, Leite RCC, Moore RS, Porto SPS, Whinnery JR. Long-transient effects in lasers with inserted liquid samples. J Appl Phys 1965;36:3–8.
[12] Sheldon SJ, Knight LV, Thorne JM. Laser-induced thermal lens effect: a new theoretical model. Appl Opt 1982;21:1663–9.
[13] Kovsh D, Hagan D, Van Stryland E. Numerical modeling of thermal refraction in liquids in the transient regime. Opt Express 1999;4:315–27.
[14] Sendhil Kaladevi, Vijayan C, Kothiyal. MP. Low-threshold optical power limiting of cw laser illumination based on nonlinear refraction in zinc tetraphenyl porphyrin. Opt Laser Technol 2006;38:512–5.
[15] Safari E, Kachanov A. Estimation of thermal lensing effect in the high-power end-pumped direct-cut crystal lasers. Opt Laser Technol 2006;38:534–9.
[16] Lancaster DG, Dawes JM. Thermal-lens measurement of a quasi steady-state repetitively flashlamp-pumped Cr, Tm, Ho: YAG laser. Opt Laser Technol 1998;30:103–8.
[17] Franko M, Tran CD. Thermal lens spectroscopy. Encyclopedia of analytical chemistry. 2010.
[18] Kitamori T, Hibara A, Tokeshi M.. Thermal lens microscopy. European Patent No. EP 1324024. Munich, Germany: European Patent Office, 2008.
[19] Harris JM, Dovichi NJ. Thermal lens calorimetry. Anal Chem 1980;52 (6):695A–706A.
[20] Sheik-Bahae M, Said AA, Wei T, Hagan DJ, Van Stryland EW. Sensitive measurement of optical nonlinearities using a single beam. IEEE J Quantum Electron 1990;26:760–9.
[21] Cuppo FLS, Figueiredo Neto AM, Gómez SL, Palffy-Muhoray V. Thermal-lens model compared with the Sheik-Bahae formalism in interpreting Z-scan experiments on lyotropic liquid crystals. J Opt Soc Am B 2002;19:1342–8.
[22] Souza RF, Alencar MARC, Meneghetti MR, Dupont J, Hickmann JM. Nonlocal optical nonlinearity of ionic liquids. J Phys.: Condens Matter 2008;20 (paper number 155102).
[23] Valencia-Loredo CE, Barrera- Rivera KA, Trejo-Durán M, Alvarado-Méndez E, Martínez Richa A, Andrade-Lucio JA., Nonlinear optical characterization of ionic liquids, nonlinear optical characterization of ionics liquids. Proceedings of SPIE, vol. 7386. Photonics North; 2009, pp. 738610 (August 04, 2009) doi: 10.1117/12.839505.
[24] Sesto, RE, Dudis DS, Ghebremichael F, Heimer NE, Low TKC, Wilkes JS., et al. Modelling synthesis and characterization of third order nonlinear optical salts. Proceedings of SPIE, vol. 5212, Linear and Nonlinear Optics of Organic Materials III; 2003, pp. 292 (November 11, 2003) doi:10.1117/12.504807.
[25] Trejo-Durán, M, Alvarado-Méndez, E, Vargas-Rodríguez, E, Estudillo-Ayala, JM, Mata-Chávez, RI., Nonlinear optical characterization of ionics liquids of 1-methylpyrrolidine family. Proceedings of SPIE 8412, Photonics North; 2012, pp. 84121X (October 23, 2012) doi:10.1117/12.2001408.
[26] Santos CE, Alencar MA, Migowski P, Dupont J, Hickmann JM. Anionic and cationic influence on the nonlocal nonlinear optical response of ionic liquids. Chem Phys 2012;403:33–6.
[27] Santos Cássio EA, Alencar MARC, Migowski P, Dupont J, Hickmann JM. Nonlocal nonlinear optical response of ionic liquids under violet excitation,. Adv Mater Sci Engi 2013:2013. http://dx.doi.org/10.1155/2013/104914 (Article ID 104914, 6).
[28] Tran CD, Challa S, Franko M. Ionic liquid as an attractive alternative solvent for thermal lens measurement. Anal Chem 2005;77:7442–7.
[29] Khosrofian JM, Garetz BA. Measurement of a Gaussian laser beam diameter through the direct inversion of knife-edge data. Appl Opt 1983;22:3406–10.
[30] Assael MJ, Antoniadis KD, Wakeham WA. Historical evolution of the transient hot-wire technique. Int J Thermophys. 2010;31:1051.
[31] Van Stryland EW, Sheik-Bahae M. In: Kuzyck MG, Dirks CN, editors. Z-scan measurements of optical and tabulations for organic nonlinear materials. New York: Marcel Dekker Inc.; 1998. p. 655–92.
[32] Mian SM, McGee SB, Melikechi N. Experimental and theoretical investigation of thermal lensing effects in mode-locked femtosecond Z-scan experiments. Optics Commun 2002;207:339–45.
[33] Falconieri M. Thermo-optical effects in Z-scan measurements using high-repetition-rate lasers. J Opt A-Pure Appl Opt 1999;1(662 -667);
Twaroski AJ, Kliger DS. Multiphoton absorption spectral using thermal blooming: I. Theory. Phys Chem 1977;20:253–8.
[34] He Guang S, Liu Song H. Physics of nonlinear optics]. Singapore: World Scientific; 1999.
[35] Karna SP, Yeates AT. Nonlinear optical materials: theory and modeling. Washington, DC: American Chemical Society; 1996; 1–22.
[36] Thermo IL. Ionic liquids database , ⟨http://ilthermo.boulder.nist.gov/ILThermo/mainmenu.uix⟩.
[37] Carrete J, Méndez-Morales T, García M, Vila J, Cabeza O, Gallego LJ, et al. Thermal conductivity of ionic liquids: a pseudolattice approach. J Phys Chem C 2012;116:1265–73.
[38] Burrell AK, Del Sesto RE, Baker SN, McCleskey TM, Baker GA. The large scale synthesis of pure imidazolium and pyrrolidinium ionic liquids. Green Chem 2007;9:449–54.
[39] Nockemann P, Binnemans K, Driesen K. Purification of imidazolium ionic liquids for spectroscopic applications. Chem Phys Lett 2005;415:131–6.
[40] Souza RF, Alencar MARC, Meneghetti MR, Hickmann JM. Large nonlocal nonlinear optical response of castor oil. Opt Mater 2009;31:1591–4.
[41] Rodríguez L, Ahn H-Y, Belfield KD. Femtosecond two-photon absorption measurements based on the accumulative photo-thermal effect and the Rayleigh interferometer. Opt Express 2009;17:19617–28.
[42] Powell RE, Roseveare WE, Eyring H. Diffusion, thermal conductivity and viscous flow of liquids. Ind Eng Chem 1941;33:430–5.